

A Model for the Tail Region of the Heliospheric Interface

V. V. Izmodenov^{1*} and D. B. Alexashov^{2**}

¹*Moscow State University, Vorob'evy gory, Moscow, 119992 Russia*

²*Institute for Problems of Mechanics, Russian Academy of Sciences,
pr. Vernadskogo 101, Moscow, 117526 Russia*

Abstract—The physical processes in the tail of the region where the solar wind interacts with a partially ionized local interstellar medium are investigated in terms of a self-consistent kinetic–gas–dynamical model. Resonant charge exchange between hydrogen atoms and plasma protons is shown to cause the contact discontinuity to disappear far from the Sun. The solar-wind plasma cools down and, as a result, the parameters of the plasma and hydrogen atoms approach the corresponding parameters of the unperturbed interstellar medium at large heliocentric distances. © 2003 MAIK “Nauka/Interperiodica”.

Key words: *solar wind, heliosphere, interstellar medium.*

INTRODUCTION

The Sun and the Solar system are known to move in a partly ionized local interstellar medium (LISM) (Lallement 1996). Direct Ulysses measurements of interstellar helium atoms (Witte *et al.* 1996) yielded the translational velocity of the Sun relative to the LISM, $\approx 25 \text{ km s}^{-1}$, and the LISM temperature, $\approx 6000 \text{ K}$. Only these two LISM parameters (velocity and temperature) can be satisfactorily determined in the solar neighborhood. Other interstellar parameters, such as the degree of ionization, the densities of the neutral and charged components, and the magnitude and direction of the interstellar magnetic field, can be determined only indirectly, by theoretically interpreting various space experiments. Indirect measurements include the backscattered solar Lyman α radiation experiments onboard the SOHO, Voyager, and Pioneer spacecraft, pickup-ion measurements onboard the Ulysses and ACE spacecraft, Voyager solar-wind measurements at large heliocentric distances, observations of Lyman α absorption toward nearby stars, and flux measurements of energetic neutral atoms (ENA). An adequate theoretical model for the solar-wind interaction with the LISM is required to properly interpret these measurements. The concept of solar-wind interaction with LISM plasma was suggested in the pioneering paper by Baranov *et al.* (1970). It has been developed for the last 30 years by several research groups [see, e.g., Izmodenov (2000, 2002) for a review].

The structure of the solar-wind–LISM interaction region is shown in Figure 1. The contact discontinuity, which is also called the heliopause (HP), separates the solar wind from interstellar plasma. The heliopause may be treated as an obstacle both to the supersonic (with a Mach number of about 10) solar wind and to the supersonic (with a Mach number of about 2) interstellar wind. Supersonic flow around an obstacle is known to be accompanied by shock formation. The supersonic solar wind passes through the termination shock (TS) to become subsonic. After the passage of the bow shock (BS), the local interstellar gas becomes subsonic. Below, the solar-wind–LISM interaction region composed of the HP, TS, and BS is called the heliospheric interface for short.

Note that when the effect of interstellar atoms is disregarded, the qualitative flow pattern in the tail region is more complex. The solar-wind flow is subsonic in the nose of the region between the termination shock and the heliopause. The flow then passes through the sonic line (Baranov and Malama 1993) to become supersonic. As a result, a complex gas-dynamical structure with a Mach disk (MD), a tangential discontinuity (TD), and a reflected shock (RS) is formed in the tail region (Fig. 1a).

The neutral interstellar component, which consists mostly of hydrogen atoms, interacts with the plasma component through charge exchange and strongly affects the locations of the discontinuity surfaces and the heliospheric-interface structure. The main difficulty in modeling the heliospheric interface is that the mean free path of neutral atoms is comparable to the characteristic size of the heliosphere. Therefore, a kinetic equation must be solved to

*E-mail: izmod@ipmnet.ru; <http://izmod.ipmnet.ru/~izmod/>

**E-mail: alexash@ipmnet.ru

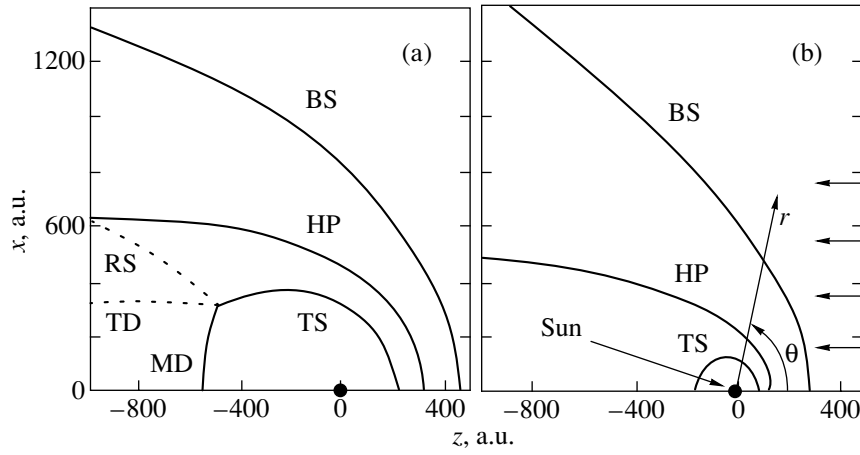


Fig. 1. The structure of the heliospheric interface: HP is the heliopause, TS is the heliospheric termination shock, BS is the bow shock, MD is the Mach disk, TD is the tangential discontinuity, and RS is the reflected shock. The right (a) and left (b) panels correspond to the calculations without interstellar hydrogen atoms and to the self-consistent solution with interstellar hydrogen atoms, respectively.

describe the motion of the neutrals. A self-consistent two-component (plasma and hydrogen atoms) model of the heliospheric interface was proposed by Baranov *et al.* (1991) and realized by Baranov and Malama (1993). The latter authors also performed the first numerical simulations of the heliospheric tail. Figure 1 shows the locations of the discontinuity surfaces with and without allowance for the effect of interstellar hydrogen atoms. The effect of atoms causes the discontinuity surfaces to approach the Sun. In the tail region, the flow structure changes qualitatively. The termination shock becomes more spherical and the Mach disk (MD), the reflected shock (RS), and the tangential discontinuity (TD) disappear (Fig. 1).

In particular, the model of the heliospheric interface allows us to answer the following two fundamental questions: (1) Where is the boundary of the Solar system? (2) How far does the influence of the Solar system on the surrounding interstellar medium extend?

To answer the first question requires defining the boundary of the Solar system. The heliopause, the surface that separates the solar wind from interstellar plasma, can be assumed to be the natural boundary of the Solar system. Note that the influence of the Solar system on the interstellar medium extends much farther than that of the heliopause. The secondary hydrogen atoms produced by charge exchange between interstellar atoms and solar-wind protons play a significant role in this influence. The mutual effects of the charge and neutral components in the heliospheric interface were studied in detail by Baranov and Malama (1993, 1995, 1996), Baranov *et al.* (1998), and Izmodenov *et al.* (1999, 2000, 2001). However, these authors focused mainly on the nose

of the heliospheric interface. At the same time, studying the heliospheric tail region is also of considerable interest. For the heliospheric tail, the definition of the heliopause as the Solar-system boundary is generally incorrect. Indeed, as can be seen from the calculations based on the Baranov–Malama model, the heliopause is not a closed surface and, hence, the solar-wind region occupies unbounded space.

Here, our goal is to study the structure of the tail region of the heliospheric interface. We focus on the charge exchange processes.

THE MODEL

To investigate the effect of charge exchange on the structure of the heliospheric tail, we used the kinetic–gas-dynamical model by Baranov and Malama (1993). In this model, the solar wind at the Earth’s orbit was assumed to be steady and spherically symmetric. The interstellar onflow was assumed to be uniform and plane-parallel. Under these conditions, the flow in the interaction region is steady and axisymmetric.

To describe the charged component (electrons and protons), we solved the hydrodynamic Euler equations with the source terms that took into account the effect of neutral atoms. The motion of interstellar atoms in the heliospheric interface was determined by solving the kinetic equation

$$\begin{aligned} & \mathbf{w}_H \cdot \frac{\partial f_H(\mathbf{r}, \mathbf{w}_H)}{\partial \mathbf{r}} + \frac{\mathbf{F}}{m_H} \cdot \frac{\partial f_H(\mathbf{r}, \mathbf{w}_H)}{\partial \mathbf{w}_H} \quad (1) \\ & = -f_H(\mathbf{r}, \mathbf{w}_H) \int |\mathbf{w}_H - \mathbf{w}_p| \sigma_{ex}^{HP} f_p(\mathbf{r}, \mathbf{w}_p) d\mathbf{w}_p \\ & + f_p(\mathbf{r}, \mathbf{w}_H) \int |\mathbf{w}_H^* - \mathbf{w}_H| \sigma_{ex}^{HP} f_H(\mathbf{r}, \mathbf{w}_H^*) d\mathbf{w}_H^* \end{aligned}$$

$$- (\beta_i + \beta_{\text{impact}}) f_H(\mathbf{r}, \mathbf{w}_H).$$

Here, $f_H(\mathbf{r}, \mathbf{w}_H)$ is the hydrogen-atom velocity distribution function; $f_p(\mathbf{r}, \mathbf{w}_p)$ is the local Maxwellian proton velocity distribution function; \mathbf{w}_p and \mathbf{w}_H are the individual velocities of the protons and hydrogen atoms, respectively; σ_{ex}^{HP} is the cross section for charge exchange between hydrogen atoms and protons; β_i is the photoionization rate; m_H is the mass of the hydrogen atom; β_{impact} is the electron impact ionization rate; and \mathbf{F} is the sum of the solar gravitational force and the radiation pressure force.

The charged and neutral components interact mainly through charge exchange, $H + H^+ \rightarrow H^+ + H$. Nevertheless, photoionization and electron impact ionization are also included in Eq. (1). The interaction between charged and neutral particles results in the exchange of mass, momentum and energy between the components. The source term $\mathbf{Q} = (q_1, q_2, z, q_{2,r}, q_3)^T$ is on the right-hand sides of the Euler equations for the charged component, where q_1 , $\vec{q}_2 = (q_{2,z}, q_{2,r})^T$, q_3 are the mass, momentum, and energy sources, respectively. The source terms are the integrals of the distribution function f_H :

$$q_1 = n_H \cdot (\beta_i + \beta_{\text{impact}}), \quad n_H = \int f_H(\mathbf{w}_H) d\mathbf{w}_H,$$

$$\vec{q}_2 = \int (\beta_i + \beta_{\text{impact}}) \mathbf{w}_H f_H(\mathbf{w}_H) d\mathbf{w}_H \quad (2)$$

$$+ \iint u \sigma_{ex}^{\text{HP}}(u) (\mathbf{w}_H - \mathbf{w}_p) f_H(\mathbf{w}_H) f_p(\mathbf{w}_p) d\mathbf{w}_H d\mathbf{w}_p,$$

$$q_3 = \int (\beta_i + \beta_{\text{impact}}) \frac{\mathbf{w}_H^2}{2} f_H(\mathbf{w}_H) d\mathbf{w}_H \quad (3)$$

$$+ \frac{1}{2} \iint u \sigma_{ex}(u) (\mathbf{w}_H^2 - \mathbf{w}_p^2) f_H(\mathbf{w}_H) f_p(\mathbf{w}_p) d\mathbf{w}_H d\mathbf{w}_p.$$

Here, $u = |\mathbf{w}_H - \mathbf{w}_p|$ is the relative atom–proton velocity.

As the boundary conditions, we assumed that the velocity of the unperturbed local interstellar flow was $V_{\text{LISM}} = 25 \text{ km s}^{-1}$ and that the LISM hydrogen-atom and proton densities were 0.2 and 0.07 cm^{-3} , respectively. The LISM temperature was taken to be 6000 K . The solar-wind velocity, density, and Mach number at the Earth's orbit were taken to be 450 km s^{-1} , 7 cm^{-3} and 10 , respectively. The hydrogen-atom velocity distribution function in the unperturbed LISM was assumed to be Maxwellian.

The Euler equations with the source term \vec{Q} were solved simultaneously with the kinetic equation for hydrogen atoms. To obtain a self-consistent solution, we used an iterative method. The kinetic equation was solved by the Monte-Carlo method with trajectory

splitting. In contrast to the previous studies based on the Baranov–Malama model, we numerically computed the solar-wind interaction with the LISM with various sizes of the tail region. In some cases, the size of the computational region reached $50\,000 \text{ AU}$ along the symmetry axis and 5000 AU perpendicular to the symmetry axis. To achieve convergence of the iterations, we used computational grids with various resolutions. The dependence of the numerical solution on outer boundary conditions was estimated by varying the extent of the tail region.

QUALITATIVE ANALYSIS

Here, we consider the effect of charge exchange ($H + H^+ \rightarrow H^+ + H$) on the plasma flow in the tail region of the heliospheric interface. The supersonic solar wind passes through the heliospheric termination shock, where its kinetic energy transforms into thermal energy. If the heliopause in the tail region is assumed to be parallel to the direction of the interstellar onflow (as follows from our numerical simulations), then the solar wind may be considered as a flow in a nozzle with a constant cross section. Our computations for the boundary conditions corresponding to the model described above show that in the case without hydrogen atoms, the solar-wind pressure downstream the termination shock in the tail region is several-fold lower than the interstellar pressure. Under these conditions, the solar-wind flow must decelerate, reaching a minimum velocity at infinity. As a result, the minimum velocity is determined only by the solar-wind parameters downstream the termination shock and by the interstellar pressure; it depends neither on the LISM density nor on the relative Sun–LISM velocity. Thus, in the case without atoms, a solution in which the solar wind (and, hence, the Solar system) extends to infinity into the heliospheric tail is possible in terms of the hydrodynamic equations. Such qualitative reasoning also remains valid when the heliopause expands or contracts, because the solar-wind flow may then be considered as a flow in an expanding or contracting nozzle.

A qualitatively different situation arises when the effect of interstellar hydrogen atoms is taken into account. Our computations show that in this case, the solar-wind pressure downstream the termination shock is higher than the interstellar pressure. The solar wind should then be accelerated by the pressure gradient. However, interstellar atoms play a significant role here. They affect the solar-wind flow through charge exchange: having mean free paths of the order of the size of the heliospheric interface, the interstellar hydrogen atoms fill its tail region. The fraction of primary (which did not undergo charge exchange in the heliospheric interface) interstellar

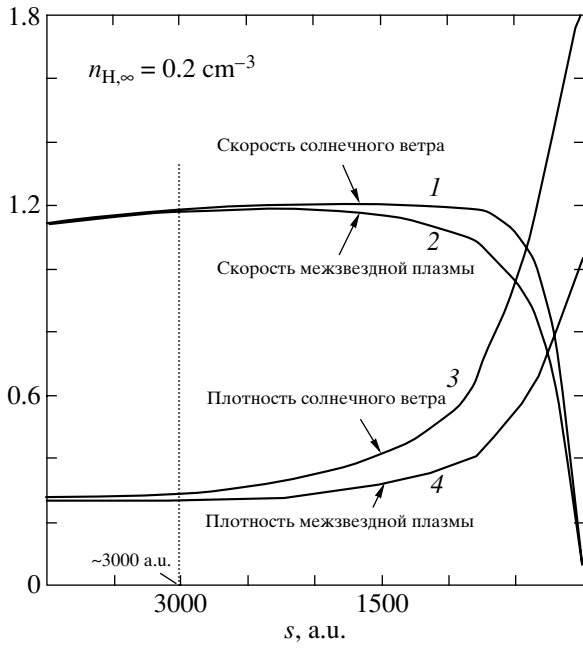


Fig. 2. The distributions of plasma velocity (curves 1 and 2) and density (curves 3 and 4) along along the contact surface. Curves 2 and 3 correspond to the interstellar medium; curves 1 and 4 correspond to the solar wind. The velocities and densities are normalized to their interstellar values; s is the heliocentric distance along the contact surface.

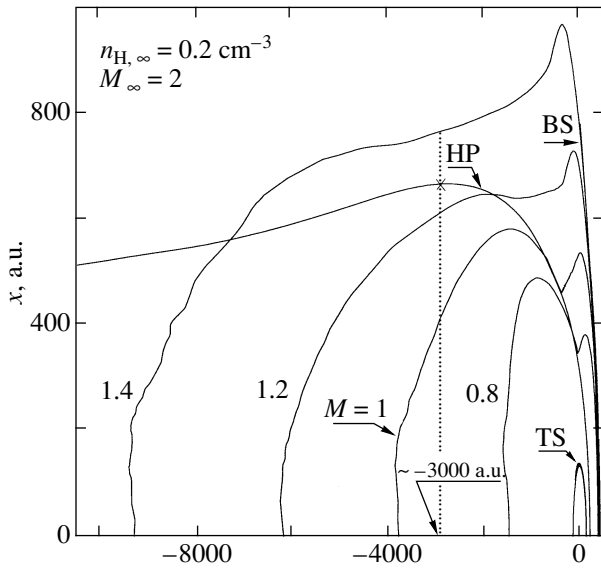


Fig. 3. Isolines of the gas-dynamical Mach number (M). The solar-wind flow is supersonic at distances larger than 4000 AU. The Mach number approaches its value in the unperturbed LISM with increasing heliocentric distance.

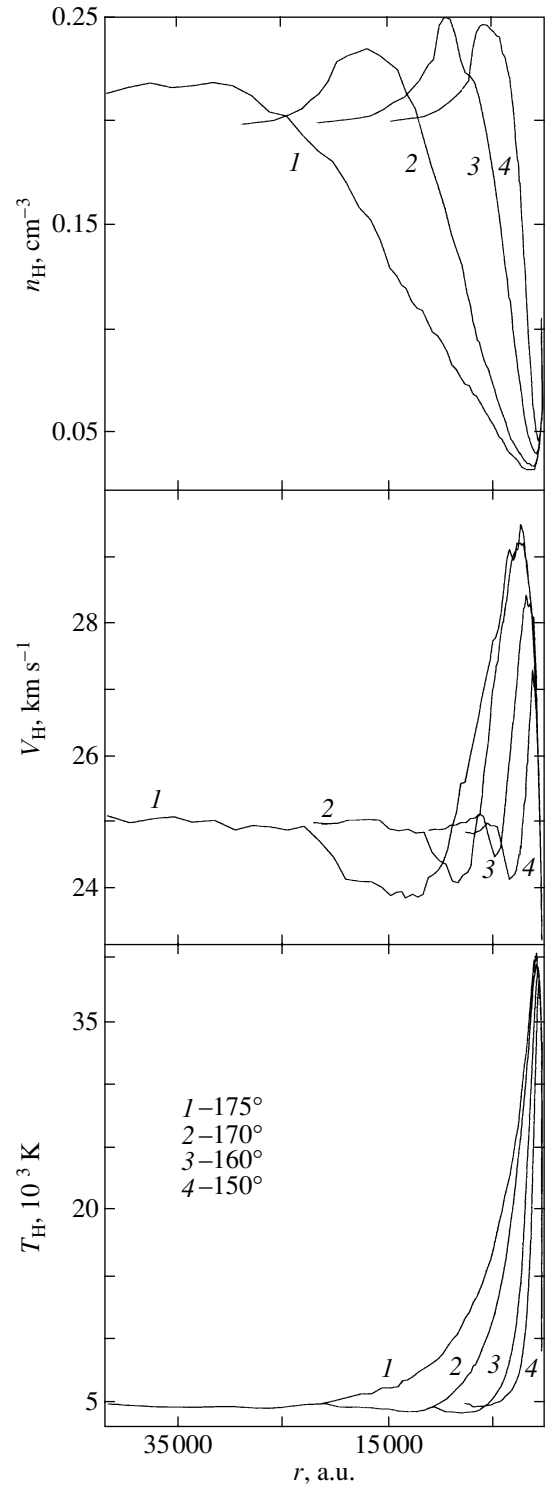


Fig. 4. The density, velocity, and temperature of the interstellar hydrogen atoms along the lines of sight with $\theta = 150, 160, 170, 175^\circ$ versus heliocentric distance r .

atoms increases with heliocentric distance. The temperature (6000 K) and velocity (25 km s^{-1}) of the primary interstellar atoms are lower than the tem-

perature (100 000 K) and velocity (100 km s^{-1}) of the post-shock solar wind. Charge exchange produces new protons with lower average and thermal velocities than those of the primary solar protons.

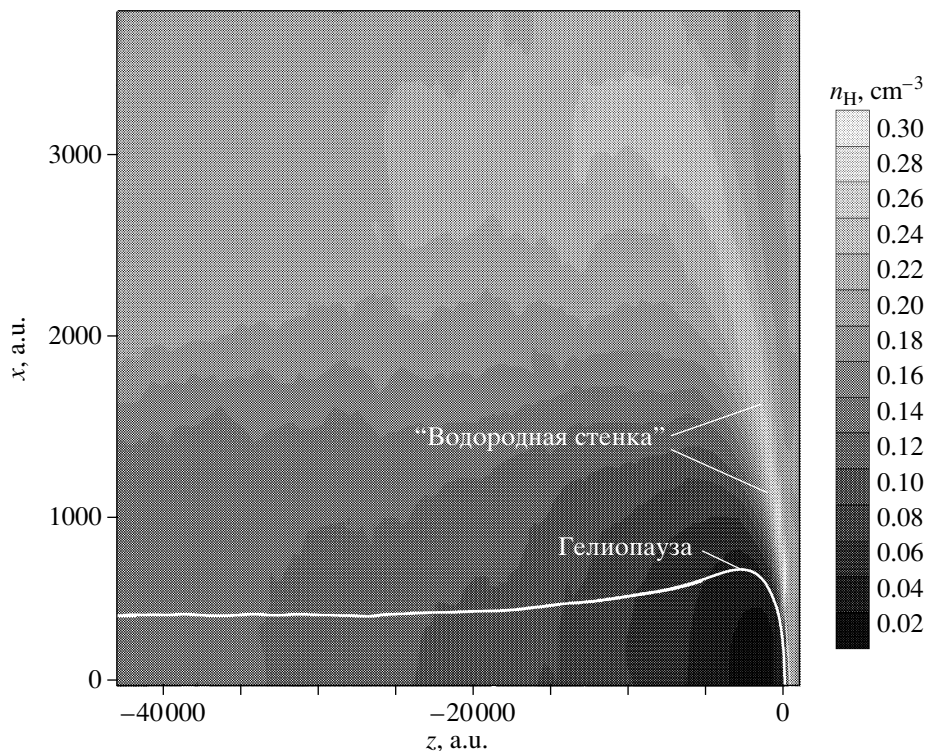


Fig. 5. The two-dimensional density distribution of hydrogen atoms in the heliospheric interface. At heliocentric distances $\sim 400\,000$ AU, the atomic density is close to its value in the unperturbed LISM. The hydrogen wall, an increase in the density of hydrogen atoms in front of the heliopause, is also seen in the figure. The intensity of the hydrogen wall decreases with increasing heliocentric distance.

Thus, charge exchange leads to effective cooling and deceleration of the solar wind. Because of the solar-wind acceleration by the pressure gradient, on the one hand, and its deceleration by charge exchange, on the other hand, the heliopause is not always parallel to the onflow direction. Since the fraction of primary interstellar atoms increases with heliocentric distance, it would be natural to expect the solar-wind velocity, density, and temperature to approach their interstellar values.

Despite many assumptions, the above qualitative analysis is confirmed by our numerical calculations. In the next section, we present and discuss the results of our numerical calculations.

RESULTS AND DISCUSSION

Our calculations confirm the above qualitative analysis. The distributions of plasma parameters in the heliotail region are shown in Figs. 2 and 3. Figure 2 presents the plasma-density and velocity distributions on both sides along the heliopause. In classical hydrodynamics, the conditions at a tangential discontinuity, which the heliopause is, are: (1) the absence of mass transport through the discontinuity and (2) pressure balance on both sides

of the discontinuity. These conditions admit a jump in density and tangential velocity when passing through the heliopause. In the presence of interstellar hydrogen atoms, momentum and energy are transferred between the solar wind and the interstellar medium via charge exchange. Therefore, the jumps in density and velocity become weaker with increasing distance calculated along the heliopause from its nose. At $z \approx -3000$ AU, where z is the distance along the symmetry axis and the minus sign denotes the direction along the LISM flow, the jumps in density and tangential velocity disappear (Fig. 2).

The plasma velocity downstream the termination shock is ≈ 100 km s $^{-1}$. This velocity then decreases as a result of charge exchange and approaches the interstellar velocity. The solar wind also effectively cools down through charge exchange. The interstellar Mach number is ~ 2 . Figure 3 shows isolines for Mach numbers in the heliospheric interface. We see that the solar wind passes through the speed of sound at $z \approx -4000$ AU. The Mach number then increases with distance from the Sun, approaching its interstellar value. The heliopause is also shown in Figure 3. The $z = -3000$ AU line indicates the boundary behind which there are no jumps in density and velocity at the heliopause.

Figures 4 and 5 present the distributions of interstellar hydrogen atoms in the heliospheric tail. Figure 4 shows the densities, velocities, and temperatures of the interstellar atoms along various lines of sight. The line-of-sight angle θ in these figures is measured from the LISM onflow direction (Fig. 1). The parameters of the hydrogen atoms approach their interstellar values at distances less than or of the order of 20 000 AU for all lines of sight. The approach is faster for smaller θ . It is also interesting to note that the hydrogen wall, an increase in the hydrogen-atom density in the region between the heliopause and the bow shock (Baranov *et al* 1991; Izmodenov 2000), is noticeable even at large $\theta \approx 150\text{--}170^\circ$. The two-dimensional distribution of hydrogen atoms in the heliospheric tail is shown in Figure 5.

Note that charge exchange significantly facilitates the numerical solution of our problem. An importance circumstance is that the solar wind becomes supersonic in the heliospheric tail, which allows us to set proper boundary conditions.

It should also be noted that here, we considered the effect of charge exchange alone. In the future, apart of charge exchange, the effects of various hydrodynamic and plasma instabilities on the flow structure should be considered. The interstellar and heliospheric magnetic fields can also affect the flow structure. Reconnection can be important as well.

CONCLUSIONS

We have studied the effect of interstellar hydrogen atoms on the structure of the heliotail region. In particular, we showed the following:

(1) Neutral hydrogen atoms qualitatively change the flow pattern of the solar wind and the LISM in the tail region via charge exchange: the termination shock becomes more spherical and the Mach disk, the reflected shock, and the tangential discontinuity disappear (Fig. 1). The discontinuities, for example, the heliopause, that exist in a purely gas-dynamical solution in the entire tail region become weaker in the solution that takes into account atoms and disappear at distances larger than 3000 AU.

(2) The parameters of the hydrogen atoms, the solar-wind plasma, and the LISM in the tail region at distances above 20 000 AU from the Sun approach their values in the unperturbed LISM because of charge exchange. This allows us to estimate the extent to which the Solar system affects the surrounding interstellar medium and, hence, to estimate

the Solar-system size in the tail region (20 000–40 000 AU). In contrast to the nose of the heliospheric interface, the Solar-system boundary in its tail region is diffusive in nature.

(3) The effect of hydrogen atoms causes the solar wind to become supersonic with increasing heliocentric distance (from 4000 AU). This removes the difficulties in specifying boundary conditions and makes it possible to obtain a proper numerical solution.

ACKNOWLEDGMENTS

We thank A.V. Myasnikov for his gas-dynamical code and Yu.G. Malama for his Monte-Carlo code. We also thank V.B. Baranov, S.V. Chalov, Yu.G. Malama, and A.V. Myasnikov for fruitful discussions. This work was supported by the INTAS (grant no. 2001-0270), the Russian Foundation for Basic Research (project nos. 01-02-17551, 02-02-06011, 02-02-06012, 01-01-00759), the CRDF (grant no. RP1-2248), and the International Space Science Institute (Bern, Switzerland).

REFERENCES

1. V. B. Baranov and Yu. G. Malama, *J. Geophys. Res.* **98** (A9), 15157 (1993).
2. V. B. Baranov and Yu. G. Malama, *J. Geophys. Res.* **100**, 14755 (1995).
3. V. B. Baranov and Yu. G. Malama, *Space Sci. Rev.* **78**, 305 (1996).
4. V. B. Baranov, K. V. Krasnobaev, and A. G. Kulikovskii, *Dokl. Akad. Nauk SSSR* **194**, 41 (1970) [*Sov. Phys. Dokl.* **15**, 791 (1971)].
5. V. B. Baranov, M. G. Lebedev, and Yu. G. Malama, *Astrophys. J.* **375**, 347 (1991).
6. V. B. Baranov, V. V. Izmodenov, and Yu. G. Malama, *J. Geophys. Res.* **103** (A5), 9575 (1998).
7. V. V. Izmodenov, *Astrophys. Space Sci.* **274**, 55 (2000).
8. V. V. Izmodenov, in *Proceedings of the Special COSPAR Colloquium in Honour of Stanislaw Grzedzielski, Leaving Executive Director of COSPAR*, COSPAR Coll. Series (2002) (in press).
9. V. V. Izmodenov, R. Lallement, and Yu. G. Malama, *Astron. Astrophys.* **342**, L13 (1999).
10. V. V. Izmodenov, M. Gruntman, and Yu. G. Malama, *J. Geophys. Res.* **106** (A6), 10681 (2001).
11. R. Lallement, *Space Sci. Rev.* **78**, 361 (1996).
12. Yu. G. Malama, *Astrophys. Space Sci.* **176**, 21 (1991).
13. M. Witte, M. Banaszekiewicz, and H. Rosenbauer, *Space Sci. Rev.* **78**, 289 (1996).

Translated by V. Izmodenov